31 January 1997

ELSEVIER

Chemical Physics Letters 265 (1997) 239–243

CHEMICAL PHYSICS LETTERS

Ion chemistry in boron trichloride BCl_3

C.Q. Jiao [1], R. Nagpal, P. Haaland

Wright Laboratory, Wright-Patterson AFB, OH 45433, USA

Received 3 June 1996; in final form 12 November 1996

Abstract

Ionization of boron trichloride by electron impact has been examined by Fourier transform mass spectrometry. The parent ion, BCl_3^+, and three fragment ions, BCl_2^+, BCl^+, and Cl^+, are observed. The total ionization cross section is $1.0 \pm 0.1 \times 10^{-15}$ cm^2 between 30 and 60 eV. BCl^+ and Cl^+ react with neutral BCl_3 to yield BCl_2^+ with bimolecular rates of $5.3 \pm 0.5 \times 10^{-10}$ cm^3 s^{-1} and $6.2 \pm 0.5 \times 10^{-10}$ cm^3 s^{-1}, respectively. BCl_2^+ does not react with BCl_3. Cl^- and Cl_2^- are produced by dissociative attachment of low-energy electrons to BCl_3, and Cl_2^- is found to rapidly react with BCl_3 to form BCl_4^-.

1. Introduction

Boron trichloride (BCl_3) is used in plasmas for etching of semiconductors [1–3], deposition or doping of boron [4,5], and in situ electric field measurements [25]. Literature reports on its electron impact ionization [7,8], attachment [9,10], scattering [11], dissociation kinetics [12] and spectroscopy [13–17] have appeared. Positive and negative ions formed by electron impact on BCl_3, and their appearance potentials have been reported [8,10,18]. Negative ions in BCl_3 discharges have also been probed with optogalvanic spectroscopy [19], and mass spectrometry [7,9].

Despite the technological interest in this molecule, and the many papers on its chemistry in plasmas, the cross sections for electron impact ionization of BCl_3 and the gas-phase ion–molecule reactions of its charged fragments have not been reported. We have quantified these collisional cross sections by Fourier transform mass spectrometry (FTMS), as we have reported previously for tetramethylsilane [20], tetraethylorthosilicate [21], and silane [22].

2. Experimental

Boron trichloride (BCl_3, 99.9%, Aldrich) was diluted with Argon (99.999% Matheson Research Grade) in a ratio of 50:50 and admitted through a precision leak valve into a modified Fourier-transform mass spectrometry (FTMS) system that has been described in detail elsewhere[23]. In brief, ions are formed by electron impact in a cubic ion cyclotron resonance (ICR) trap cell at pressure in the 10^{-7} Torr range. An electron gun (Kimball Physics ELG2, Wilton, NH) irradiates the trap with a few hundred picoCoulombs of low-energy electrons. The ions' motions are constrained radially by a superconducting solenoidal magnetic field of $\approx$ 2 T and axially by a

[1] Author to whom correspondance should be addressed at Mobium Enterprises, Inc., 3055 Rodenbeck Dr., Beavercreek, OH 45432, USA.

PII S0009-2614(96)01419-4

nominal (≈ 2 V) electrostatic potential applied to the trap faces that are perpendicular to the magnetic field. Ions of all mass-to-charge ratios are simultaneously and coherently excited into cyclotron orbits using a radiofrequency voltage applied to two opposing trap faces that are parallel to the magnetic field [24,25]. Following cyclotron excitation, the image currents induced on the two remaining faces of the trap are amplified, digitized, and Fourier analyzed to yield a mass spectrum.

Calculation of cross sections from the mass spectrum requires knowledge of the gas pressure, the electron beam current, and the number of ions produced. These calibration issues have been described previously [23,26]. The ratio of BCl_x^+, Cl^+ : Ar^+ signals gives cross sections relative to the well-known cross sections for argon [27,28] ionization since the BCl_3 : Ar pressure is known. As a cross-check, and for ion–molecule kinetic analyses, the gas pressure is calibrated using a pulsed valve and a spinning rotor friction gauge (MKS Instruments model SRG2, Burlington, MA) with the vacuum chamber isolated from the pumps by closed gate valves. Electron current is collected on a Faraday cup and recorded with a digital oscilloscope after passage of the electron beam through the ion trap. The quantitative relationship between the image current and the number of ions is based on a lengthy, but elementary, solution of Maxwell's equations for the cubic ICR cell. This is required to quantify both excitation of the ions and detection of the resulting image current [23].

The distribution of electron energies in the trap, based on solution of Laplace's equation for the experimental geometry, is roughly Gaussian with a full width at half maximum of 0.5 eV due to the electrostatic trapping bias [23]. The energy scale is accurate to ± 0.5 eV based on comparison of noble gas ionization thresholds with spectroscopic data. We fit the cross-section data to a heuristic but parsimonious functional form:

$$\sigma(\epsilon - T) = A \times \tanh \frac{\pi * (\epsilon - T)}{\alpha} \times e^{-k(\epsilon - T)},$$

where σ is the cross section, ϵ is the electron energy, T is the appearance potential, A scales the amplitude, k characterizes the higher energy behavior of σ, and α quantifies $d\sigma/d\epsilon$ near threshold.

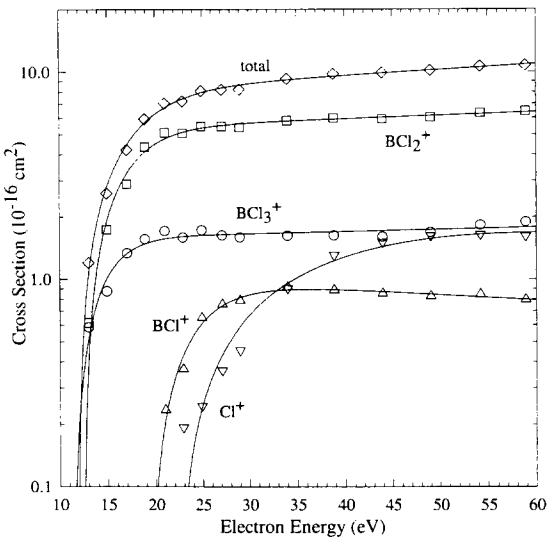

Fig. 1. Cross sections (cm^2) for ionization of BCl_3 by electron impact. Points represent experimental data. Solid lines are fits of the equation described in the text.

3. Results and discussion

Ionization cross-sections for BCl_3 are shown in Fig. 1, while parameters for functional fits to the observed cross-sections are summarized in Table 1. A striking feature of the data is the observation of the molecular ion, BCl_3^+, in substantial yield. In a recent paper on ionization in plasmas containing BCl_3 [7], no BCl_3^+ in the amplitude modulated discharge mass spectra was reported. We conclude that the BCl_3 has been substantially consumed by reactions with electrons, ions, surfaces, and neutral radicals during the long residence time of the gas in these plasmas. This conclusion is reinforced by the absence of B^+ in the FTMS spectra of BCl_3 and its presence in the amplitude modulated plasma spectra shown in reference [7]. We ascribe the observation of B^+ to dissociative ionization of species other than BCl_3 that are produced in the radiofrequency discharge [7].

The present results also update the observations in reference [8] where both B^+ and Cl_2^+ were reported in the mass spectra of BCl_3. The above work correctly attributed the formation of the latter to an artifact of pyrolysis on the ionizer filament. The present data show neither B^+ nor Cl_2^+ because pyrolysis is precluded by the 2 meter distance between the filament and ion trap. We propose that the observation of B^+ in reference [8] is likewise a consequence of filament pyrolysis.

Table 1
Fitting parameters for simple and dissociative ionization cross sections. Also shown are appearance potentials estimated from thermochemical data in the JANAF tables

Ion	A (cm^2)	k (eV^{-1})	α (eV)	T (eV)	JANAF T (eV)
BCl_3^+	1.6×10^{-16}	-2.4×10^{-3}	15	11.4	11.6
BCl_2^+	5.3×10^{-16}	-3.8×10^{-3}	21	12.5	12.4
BCl^+	1.0×10^{-16}	5.9×10^{-3}	24	19.4	19.5
Cl^+	2.4×10^{-16}	6.7×10^{-3}	80	22.3	26.7

The most abundant positive ion from threshold to 60 eV is BCl_2^+. By introducing a time delay between ion formation at 25 eV and ion cyclotron excitation and detection, we track the reactions of ion fragments with BCl_3 as shown in Fig. 2. The more extensively dissociated ions BCl^+ and Cl^+ react with BCl_3 to produce BCl_2^+ at rates of 5.3 ± 0.5 and $6.2 \pm 0.5 \times 10^{-10}\,cm^3 s^{-1}$, respectively. The Ar^+ ion also reacts rapidly:

$$Ar^+ + BCl_3 \rightarrow BCl_2^+ + (Ar, Cl)$$
$$k = 5.0 \pm 0.5 \times 10^{-10}\ cm^3\ s^{-1}.$$

Based on the published value for the polarizability of BCl_3, $\alpha = 9.38 \times 10^{-24}\ cm^3$ [29], these reactions occur at about one-half of the Langevin limiting value. The reaction rates of BCl_x^+ with BCl_3 are the same whether the ions were formed by 25 eV or 50 eV electron impact. The depletion of Cl^+ is about 1.5 times faster at 50 eV, but our data cannot resolve whether this rate increase is attributable to spin-orbit, electronic, or translational excitation of the reactant Cl^+ ion at 50 eV.

Small quantities of HCl are observed, either from impurities in the BCl_3 cylinder, or as products of the reaction between BCl_3 and traces of water in the vacuum manifolds. We also observe the production of $BClOH^+$ that arises either from reaction of water vapor with BCl_3^+:

$$BCl_3^+ + H_2O \rightarrow BClOH^+ + (H, 2Cl)$$

or dissociative charge transfer to hydrolyzed BCl_3 :

$$BCl_3 + H_2O \rightarrow BCl_2OH + HCl,$$
$$(Ar^+, BCl_3^+) + BCl_2OH \rightarrow BClOH^+ + Cl + (Ar, BCl_3).$$

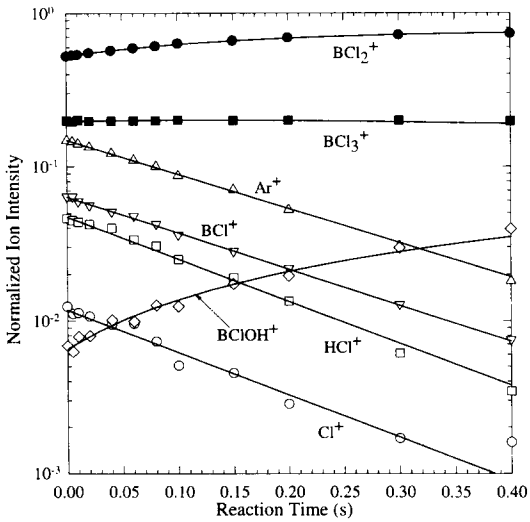

Fig. 2. Time evolution of positive ion species produced by 25 eV electron impact at a BCl_3 pressure of 3.2×10^{-7} Torr. Traces of HCl^+ are attributed to the reaction of BCl_3 with background water vapor. Points represent experimental data. Solid lines are fits of a kinetic model which gives the reaction rate coefficients presented in the text.

No $BClOH^+$ was observed in kinetic experiments during which all ions but BCl_2^+ were ejected.

Negative ions from electron attachment to BCl_3 were first examined between 10 and 60 eV. No anions attributable to direct dissociative attachment at these energies were observed. However, secondary electrons from positive ionization were trapped in the ICR cell, and these electrons produced substantial quantities of Cl^- and Cl_2^-. No boron-containing anions were observed by the secondary electron attachment.

In order to study dissociative attachment of electrons to BCl_3 at energies below 10 eV, we studied the negative ion intensities as a function of applied trapping potential. The results are shown in Fig. 3 at a primary electron energy of 50 eV. We note that the range of secondary electron energies in the trap is constrained both by their kinetic energy following ionization and by the applied trapping potential. As the trapping potential increases the mean energy of trapped secondary electrons rises, leading to increased dissociative attachment as shown in Fig. 3. We infer that the secondary electrons from positive ionization were trapped in the ICR cell, and dissociative attachment by these electrons produced substantial quantities of Cl^-

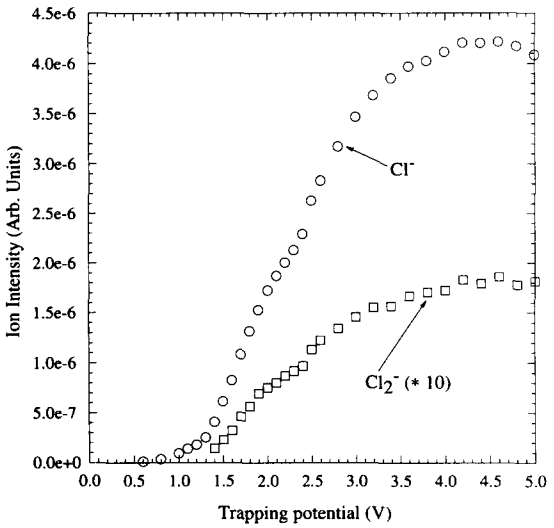

Fig. 3. Negative ion yields from trapped secondary electrons as a function of the applied trap bias. The primary electron energy is 50 eV.

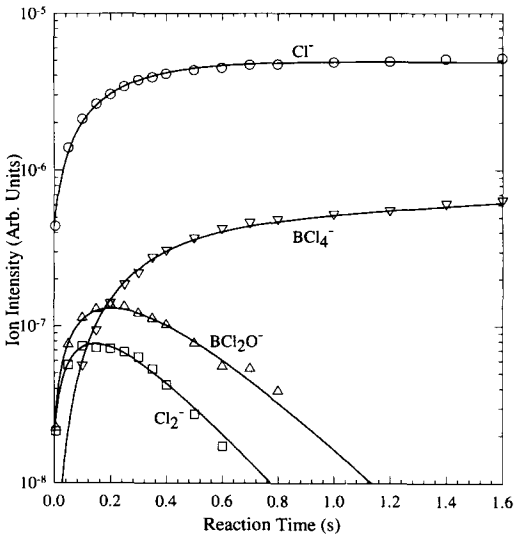

Fig. 4. Negative ion yields as a function of time delay between the generation of secondary electrons in the trap and the observation time. The increase in ion concentration over the first ≈ 400 ms is due to the attachment of trapped secondary electrons.

and Cl_2^-. The above conclusion is reinforced by the observation of negative ion production after cessation of the electron beam, as shown in Fig. 4. Although the energy resolution of our experiment is inferior to that of conventional crossed beam measurements for electron energies below 10 eV, we identify the low-energy attachment resonances and their product ions by FTMS.

Due to uncertainties in the number and in the energy distribution of trapped secondary electrons, the data summarized in Fig. 4 do not permit derivation of the rate coefficients for negative-ion molecule reactions. However, the data do reveal three features of anion chemistry in BCl_3. First, Cl_2^- reacts rapidly with BCl_3:

$$Cl_2^- + BCl_3 \rightarrow BCl_4^- + Cl$$

but the rate for the Cl^- reaction:

$$Cl^- + BCl_3 \rightarrow BCl_4^-$$

is substantially slower. At present we cannot say whether the product BCl_4^- (from the latter reaction) is stabilized by emission of radiation or by a combination of a long vibrational lifetime and collisional quenching at $\approx 10^{-6}$ Torr. Second, the ion–molecule reaction:

$$Cl^- + BCl_3 \rightarrow Cl_2^- + (B, 2Cl)$$

is not observed, indicating that Cl_2^- is produced only by the dissociative attachment of electrons to BCl_3. Both Cl^- and Cl_2^- were reported in drift-dwell-drift electron swarm experiments [18] but later quadrupole mass spectrometry of BCl_3 plasmas reported only Cl^- [9]. Finally, the data in Fig. 4 show that BCl_2O^- is formed by dissociative attachment to an impurity neutral such as BCl_2OH, rather than by a negative-ion molecule reaction. The formation of BCl_2OH is consistent with our observation of $BClOH^+$ in the cation kinetics experiments, and with a mechanism by which BCl_3 is proposed to scavenge oxygen in discharges [30].

4. Conclusions

Electron impact ionization of BCl_3 yields BCl_2^+, BCl_3^+, BCl^+, and Cl^+ with a total cross section of $1.0 \pm 0.1 \times 10^{-15}$ cm^2 between 30 and 60 eV. Ion–molecule reactions of BCl^+ and Cl^+ yield BCl_2^+ with rate constants of 5.3 ± 0.5 and $6.2 \pm 0.5 \times 10^{-10}$ cm^3 s^{-1}, respectively. Dissociative attachment of low-energy electrons to BCl_3 yields primarily Cl^- with smaller quantities of Cl_2^-. No boron-containing ions are found by dissociative attachment, but both Cl^- and Cl_2^- re-

act with BCl_3 to produce BCl_4^-. No further clustering of BCl_4^- is observed. We infer that heavier anions observed by mass spectrometric sampling from BCl_3 plasmas are a result either of attachment to higher molecular weight species formed in the plasma or to reactions of anions with neutral radicals that are precluded at the pressures and charge densities used in the FTMS experiments.

Acknowledgements

The authors wish to thank Dr. Alan Garscadden for stimulating discussions and critical reviews, and the Air Force Office of Scientific Research for financial support.

References

[1] D.L. Flamm and V.M. Donnelly, Plasma Chem. Plasma Proc. 1 (1981) 317.
[2] J.W. Coburn, Plasma Chem. Plasma Proc. 2 (1982) 1.
[3] K.E. Greenberg, G.A. Hebner and J.T. Verdeyen, Appl. Phys. Lett. 44 (1984) 299.
[4] L.E. Kline, in: Nonequilibrium effects in ion and electron transport, eds. J.W. Gallagher, D.F. Hudson, E.E. Kunhardt and R.J. Van Brunt (Plenum, New York, 1990).
[5] A. Slaovi, F. Foulan, L. Fuchs, E. Foganassy and P. Siffert, Appl. Phys. A 50 (1990) 317.
[6] R.A. Gottscho, Phys. Rev. A 36 (1987) 2233.
[7] L.J. Overzet and L. Luo, Appl. Phys. Lett. 59 (1991) 161.
[8] J. Marriott and J.D. Craggs, J. Electron. Control 3 (1957) 194.
[9] Z.Lj. Petrovic, W.C. Wang, M. Suto, J.C. Han and L.C. Lee, J. Appl. Phys. 67 (1990) 675.
[10] I.S. Buciel'nikova, Sov. Phys. JETP 35 (1959) 783.
[11] R. Nagpal and A. Garscadden, Appl. Phys. Lett. 64 (1994) 1626.
[12] G.R. Scheller, R.A. Gottscho, T. Intrator and D.B. Graves, J. Appl. Phys. 64 (1988) 4384.
[13] Z.J. Jabbour, K.E. Martus and K. Becker, Z. Phys. D 9 (1988) 263.
[14] M. Suto, C. Ye, J.C. Han and L.C. Lee, J. Chem. Phys. 89 (1988) 6653.
[15] L.C. Lee, J.C. Han and M. Suto, J. Chem. Phys. 91 (1989) 2036.
[16] P.G. Gilbert, R.B. Siegel and K. Becker, Phys. Rev. A 41 (1990) 5594.
[17] F.W. Breitbarth, Plasma Chem. Plasma Proc. 12 (1992) 261.
[18] J.A. Stockdale, D.R. Nelson, F.J. Davis and R.N. Compton, J. Chem. Phys. 56 (1972) 3336.
[19] R.A. Gottshco and C.E. Gaebe, IEEE Trans. Plasma Sci. PS-14 (1986) 92.
[20] S. McGinnis, K. Rielh and P.D. Haaland, Chem. Phys. Lett. 232 (1994) 99.
[21] J. Holtgrave, K. Riehl, D. Abner and P.D. Haaland, Chem. Phys. Lett. 215 (1993) 548.
[22] P.D. Haaland, J. Chem. Phys. 93 (1990) 4066.
[23] K. Riehl, Collisional detachment of negative ions using FTMS, Ph.D. Thesis, Air Force Institute of Technology (1992).
[24] A.G. Marshall, T.L. Wang and T.L. Ricca, J. Am. Chem. Soc. 107 (1985) 7893.
[25] S. Guan, J. Chem. Phys. 91 (1989) 775.
[26] P.D. Haaland, Chem. Phys. Lett. 170 (1990) 146.
[27] R.C. Wetzel, F.A. Baiocchi, T.R. Hays and R.C. Freund, Phys. Rev. A 35 (1987) 559.
[28] E. Krishnakumar and S.K. Srivastava, J. Phys. B: At. Mol. Opt. Phys. 21 (1988) 1055.
[29] R.C. Weast, ed., CRC Handbook of Chemistry and Physics, 66th Ed. (CRC Press, Boca Raton, 1985).
[30] K. Tokunaga, F.C. Redeker, D.A. Danner and D.W. Hess, J. Electrochem. Soc. 128 (1981) 851.